



# Strength Properties of Geopolymer Concrete Modified with Recycled Aggregates

Anandh Babu Malayali<sup>1</sup> · Ramesh Babu Chokkalingam<sup>1</sup> · M. Muthukannan<sup>1</sup>

Received: 31 December 2020 / Accepted: 18 May 2021 / Published online: 3 June 2021  
© Shiraz University 2021

## Abstract

The main goal of this paper is to investigate the effects of recycled aggregates in geopolymer pervious concrete (GPC). The usage of recycled aggregate (RA) in the construction field is getting more attention nowadays due to sustainable construction methods. In this study, natural aggregates (NA) are partially replaced with recycled aggregates such as recycled concrete aggregate and recycled brick aggregate (RBA) in geopolymer pervious concrete. For preparing geopolymer, ground granulated blast furnace slag (GGBS) was used in this investigation. Activators such as 12 M sodium hydroxide and sodium silicate solutions were used to synthesize the geopolymer concrete in this investigation. The sodium silicate-to-sodium hydroxide ratio was maintained at 2.5 throughout this study. Mechanical and durability properties of GPC were determined as per Indian standards. The effects of RA in geopolymer pervious concrete were briefly investigated. It has been observed that durability properties are affected by the incorporation of recycled aggregate (RA) in geopolymer concrete. The compressive strength value of RC12 is less than that of GC12 and RB12 is less than that of RC12. The strength properties of structural beam elements were reduced due to the incorporation of recycled concrete and recycled brick aggregate in geopolymer concrete; at the same time, the reduction always lies in acceptable ranges. Validation was done using ANSYS software. This paper leads the utilization of recycled aggregates in GGBS-based GPC instead of NA at ambient curing condition.

**Keywords** Geopolymer pervious concrete · Ground granulated blast furnace slag (GGBS) · Recycled brick aggregate (RBA) · Recycled concrete aggregates (RCA)

## 1 Introduction

Scarcity of natural aggregates is a major concern in the construction industry due to its limited availability and also the restrictions by the government in mining the aggregates only for a certain depth citing environmental concerns. Hence, there is a need to look for alternate aggregates for concrete production. Also, there were concerns that most of the lands were covered with concrete which make the surface impermeable to rainwater into the ground. Also, construction waste worldwide accounts for 40% which is considered as construction demolition waste (CDW) (Mehta 2001; Noushini and Castel 2016; Somna et al. 2011). From the previous studies, the amount of CDW produced in Australia,

China, and mainland accounts to be 44%, 40%, and 29% respectively (Poon et al. 2012; Yuan et al. 2012; McDonald 1996). The enormous quantity of concrete waste formed can be utilized as aggregates in concrete are a healthy conventional management approach. In 2009, construction demolition waste (CDW) was formed with almost 170 million tons in the United States Environmental Protection Agency reported (US Environmental Protection Agency (USEPA) 2009). Details reported that 56% of concrete waste was available in total solid waste formed in Florida (Cochran et al. 2007). Concrete developed using recycle aggregate leads to reducing the concrete waste landfills and resulting protection of landfill areas (Akbarnezhad et al. 2013; Akbarnezhad and Nadoushani 2015; Poon et al. 2004; Etxeberria et al. 2007; Limbachiya et al. 2012; Tangchirapat et al. 2008). Previous studies showed the recycled concrete aggregate (RCA) and recycled brick aggregate (RBA) were possible sources of replacement of natural aggregate, but the mechanical properties of RCA and or RBA are substandard to conventional concrete (Khalaf and DeVenny 2004;

✉ Anandh Babu Malayali  
anandhcivil@gmail.com

<sup>1</sup> School of Environmental and Construction Technology,  
Kalasalingam Academy of Research and Education,  
Srivilliputhur, India

Khalaf and DeVenny 2005; Limbachiya et al. 2000, Lotfy and Al-Fayez 2015). Compressive strength was found to be reduced in concrete fabricated using RCA/RBA aggregate compared to NA-based concrete (Debieb and Kenai 2008). When 100% of NA replacement with Recycled aggregate in cement concrete which shows that 30% of reduction in compression strength (Yang et al. 2011). Pervious concrete is a mixture of coarse aggregates and cement. Due to fine aggregate absence and need of voids content, the workability decreases on fresh concrete (Meininger 1995; Ghafoori and Dutta 1995; Babu and Babu 2017). To achieve the desired strength and permeability, the successful void material must be optimized. In previous concrete, the effective void content usually varies from 15 to 35 percent. Monitoring the degree of compaction effort as well as the aggregate ratios and properties will help reach the required void content (Varol et al. 2020) (Cetin 2013). The information of two types of research was summarized that are reported pervious concrete having exceptionally high water pollutant removal rates. Pervious concrete removed 82 and 95 percent gross dissolved solids in experiments conducted in Virginia and Maryland, respectively. Increased void ratios increase penetration rates but reduce compressive strength considerably. Porosities ranging from 15 to 25% are suggested (Tennis et al. 2004). Water-to-cement ratios of 0.27–0.30 are most widely used, according to reports. Water and air will continue to flow through the matrix into the subsoil beneath, leading to the porous structure. Because of the pore sizes, pervious concrete not only eliminates runoff but also serves as a barrier by rotting and trapping pollutants (such as oils and debris) on and inside the framework (Schaefer et al. 2006). The variation and size of aggregate in the mix, the amount of water and cement applied, and the degree of compaction all influence the size of these pores. Pervious concrete pavements have better hydraulic absorption than traditional concrete pavements, resulting in quieter pavements. The porous nature of the material contributes to superior hydraulic absorption (Neithalath et al. 2006). Pervious fly ash-based geopolymer concrete is higher compression strength compared to cement binder-based conventional concrete (Tho-in et al. 2012). The production of cement emits CO<sub>2</sub> into the atmosphere, which results in global warming. Every year, 7% CO<sub>2</sub> is emitted by cement factories all around the world (Mehta 2001). One tonne production of cement releases one tonne of CO<sub>2</sub> into the atmosphere (Malhotra and Meht 2002). The production of fly ash-based geopolymer requiring 60% less energy and 80% of CO<sub>2</sub> emission compared with OPC production (Duxson et al. 2007) was estimated. Geopolymer concrete is one such concrete in which the cement is fully replaced with supplementary cementitious materials. Geopolymer is the term introduced by Davidovits (1991). Ground granular blast furnace slag-based pervious geopolymer concrete also shows higher strength compared to geopolymer fly ash-based and

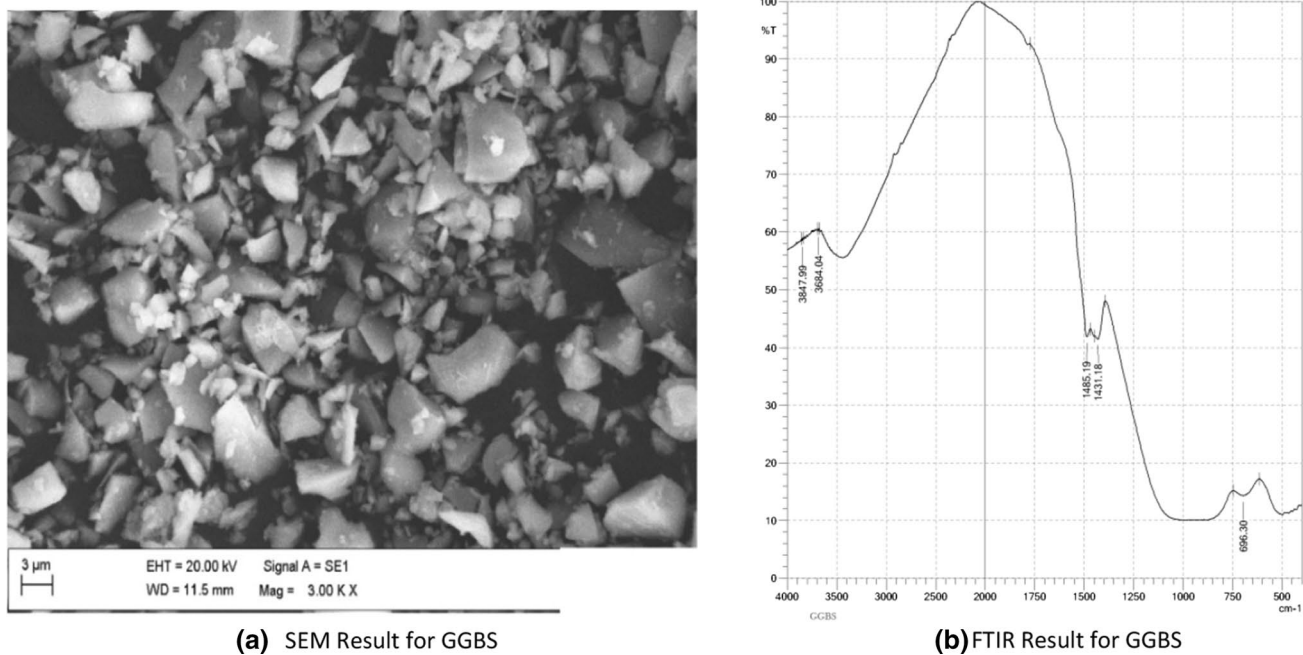
cement binder-based pervious concrete (Malayali et al. 2019). Geopolymer concrete has the properties of high early strength, admirable mechanical and durability properties compared with cement concrete, respectively (Chindaprasirt and Chalee 2014; Malayali et al. 2020). Based on the previous literature, it has been identified that there has been limited work done on GGBS-based geopolymer pervious concrete. Also, usage of recycled aggregate in geopolymer pervious concrete is minimal. Hence, in this research, we have studied the mechanical, durability, structural element flexural properties and analysis done in ANSYS of GGBS-based geopolymer recycled pervious concrete.

## 2 Materials Used

GGBS (ground granulated blast furnace slag) from a locally available vendor was used in this investigation. Scanning electron microscopy (SEM) was carried out in GGBS material which shows particles having sharp edges (Celen et al. 2019) (Wen et al. 2019) which increases the binding nature, and Fourier transform infrared spectroscopy was used to identify the infrared spectrum of emission or absorption of powder stage tested. Wavelength lies in the middle IR-region silicon carbide element limited to long wavelength 2000 cm<sup>-1</sup>. Properties of coarse aggregate are identified based on standard shown in Fig. 1. Building materials are not having or very less natural radioactivity properties (Mavi and Akkurt 2010) (Akkut et al. 2010) (Akkurt and Akyildirim 2012). In this paper, three different nominal sizes of coarse aggregates such as natural, recycle concrete aggregate, and recycle brick aggregate (Akkut et al. 2006), such as 6 mm, 12 mm, and 20 mm, were used with the research work properties, which are listed in Table 1. Demolished building waste is divided into concrete and brick which is crushed in a crusher to produce the required size utilized as aggregate shown in Fig. 2. Recycled concrete aggregates and recycled brick aggregates are also used as a replacement for natural aggregates (Cetin 2015a, Book Chapter 55). The molarity of NaOH was fixed at 12 M based on the previous work on geopolymer concrete (Malayali et al. 2019; Malayali et al. 2020).

## 3 Mix Proportions and Casting

All pervious geopolymer concrete was produced with GGBS and coarse aggregate ratio of 1:3. Ratios of Na<sub>2</sub>SiO<sub>3</sub>/NaOH and alkali liquid were kept constant at (2.5) throughout the investigation, and liquid-to-binder ratio plays the main role in polymerization (Kilincarslan et al. 2006). Three different aggregate sizes of 6 mm, 12 mm, and 20 mm were used for making geopolymer



(a) SEM Result for GGBS

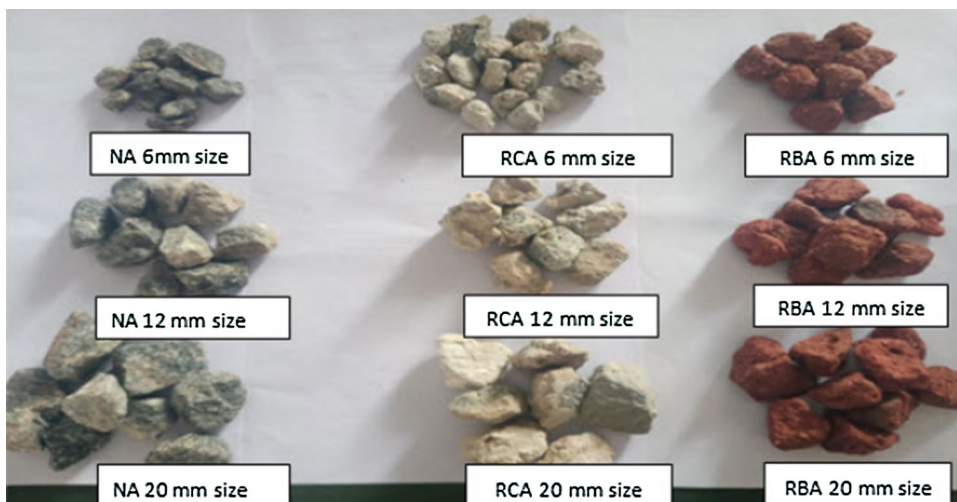
(b) FTIR Result for GGBS

Fig. 1 GGBS

Table 1 Aggregate characteristics

Properties	Natural aggregate			Recycled concrete aggregate			Recycled brick aggregate		
	6	12	20	6	12	20	6	12	20
Size of the aggregate (mm)	6	12	20	6	12	20	6	12	20
Specific gravity	2.7	2.8	2.8	2.46	2.6	2.68	2.02	2.1	2.14
Density (kg/m <sup>3</sup> )	1580	1560	1490	1484	1404	1365	985	958	911
Impact value (%)	24.15	17.23	11.58	26.15	25.35	24.65	29.17	28.65	26.58

Fig. 2 Aggregates



pervious concrete. Total numbers of mixes are nine, three with natural aggregate utilized geopolymer concrete (GC), three with recycled concrete aggregate utilized

geopolymer recycled concrete aggregate concrete (RC), and three with recycled brick aggregate utilized geopolymer recycled brick aggregate concrete (RB) which

cube cast 162 numbers, cylinder cast 135 numbers, and beam cast 27 numbers a total number of samples 324 cast (Fig. 3) and experiments done. The mix proportions and their details are listed in Table 2.

## 4 Testing Methods

### 4.1 Strength and Durability Studies

Compressive strength, split tensile strength, and density of the concrete are the major tests performed in this investigation. A compressive test was conducted based on the guidelines given in IS 516 (1959), split tensile test was measured by following guidelines given in IS 5816 (1999), and density of concrete was measured based on the guidelines specified in ASTM C642-13 (2013). The compressive strength depends on the aggregate size (Malayali et al. 2019). Voids in concrete specimens and the water permeability were measured by the following methods presented in IS 3085 (1965). Void ratio is calculated based on IS 2386-3 (1963) using Eq. (1)

$$V = \frac{1 - (W2 - W1)X100}{\rho_w \text{Vol}} \quad (1)$$

where  $V$  is the void ratio,  $W1$  is the weight of the specimen underwater in gms,  $W2$  is the saturated weight of the specimen gms,  $\rho_w$  is the density of water, and  $\text{Vol}$  is the volume of the specimen. After conducting the void ratio test, specimens are placed over the apparatus, which measures the permeability values of the specimens. Water absorption plays an essential role in concrete (Malayali et al. 2020). The water permeability coefficient is calculated by using Darcy's law with the help of Eq. (2)

$$K = \frac{QL}{HA t} \quad (2)$$

where  $k$  is the coefficient of water permeability (cm/s),  $Q$  is the quantity of water collected (cm<sup>3</sup>) over time  $t$  (s),  $L$  is the length of specimen (cm),  $H$  is the water head (cm), and  $A$  is the cross-sectional area of the specimen (cm<sup>2</sup>). The permeability testing machine is shown in Fig. 4.

The samples water absorption tests were conducted to determine the overall capacity of the untreated and treated geopolymer concrete to absorb water. It was assessed in

Fig. 3 Specimens casted



Table 2 Mix proportions

Specimen ID	GGBS (Kg/m <sup>3</sup> )	Recycled aggregates (Kg/m <sup>3</sup> )	Natural aggregates (Kg/m <sup>3</sup> )	NaOH	Na <sub>2</sub> SiO <sub>3</sub>
GC6	450	Nil	1350	33	66
GC12	450	Nil	1350	33	66
GC20	450	Nil	1350	33	66
RC6	450	1360	–	41	105
RC12	450	1360	–	42	106
RC20	450	1360	–	43	107
RB6	450	1360	–	44	108
RB12	450	1360	–	45	109
RB20	450	1360	–	46	110



Fig. 4 Permeability testing equipment

accordance with the Standard EN 13755 (2008). The specimens were mounted in a container containing boiling water (to extract dissolved gases) at a room temperature of  $\sim 22\text{ }^{\circ}\text{C}$  and a level hitting half the height after being dried to constant weight in the early stage. After one hour,  $3/4$  of height water is slowly applied and then after two hours to complete immersion at the height of  $25 \pm 5\text{ mm}$ . After 48 h, the samples were separated from the water, wiped with a soft cloth, and easily measured. The test was performed for five specimens, and readings were obtained on average. The water absorption percentage value is calculated using Eq. (3)

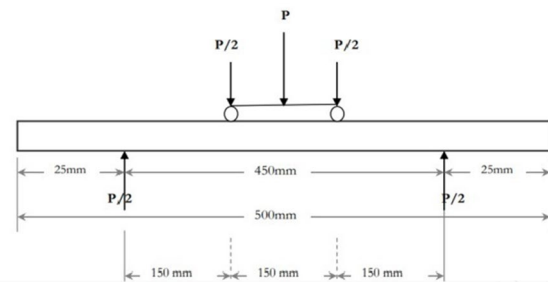
$$A = \frac{m_w - m_d}{m_d} \times 100(\%) \quad (3)$$

where  $A$  is the total water absorption (%),  $m_d$  is the weight of oven-dried sample in the air in gram, and  $m_w$  is the weight of the sample saturated with water in gram.

Before conducting the sorptivity tests, the samples were preconditioned for seven days at  $500\text{ }^{\circ}\text{C}$ , and these specimen edges were sealed with wax or organic compound with 50:50 proportion. Sealing is essential to realize the simplex flow of the specimen. Initial weight was measured after waterproofing was done. The specimens were taken at 30 min, 60 min, 90 min, and 120 min, and the specimens were wiped with the cloth to remove excess water. Now the samples were weighed, and the sorptivity values were



(a) Flexural test Setup Two-point Load condition



(b) Schematic diagram Flexural test Setup Two-point Load condition

Fig. 5 Flexural test setup

tabulated. Depending upon the velocities, the material properties are defined. When the standard of concrete is good in terms of density, durability, and homogeneity, then the permeability speed is higher on the concrete surface.

## 5 Tests on Beam

The beam size of  $100 \times 100 \times 500\text{ mm}$  was fabricated using beam molds and cured. A three-point loading method was used to test the beam using a 500-kN loading frame. Dial gauges of least count 0.001 mm were placed at the tension face to measure the deflection along the length. Three numbers of dial gauges of least count 0.002 mm were placed to measure the surface strains (Fig. 5a, b). A Brinell microscope is a device used to measure crack width, and the least count of the microscope is about 0.01 mm and measure scale for reference measurement. Hydraulic Jack is used to apply the load at the rate of 2 kN, and the deflection is measured using dial gauges. After the first crack, the width of the crack was measured for a 10-kN interval. The loading of the beam was continued until the failure of the beam. Ultimate load, critical load, and service load of the specimen were noted by conducting the loading test, and the results are tabulated.

## 6 Experimental Results

The compressive strength, split tensile strength values, and density are listed in Table 3. Under ambient curing, compression strength shows higher GGBS-based geopolymer concrete (Venkatesan and Pazhani 2016). The compressive strength values range from 0.952 to 7.59. The best value of compressive strength is observed in GC12 specimens in which the void spaces are moderate; thus, the strength values are reasonably good when compared to the other specimens. At the same time, 6-mm aggregate containing GC exhibited lower strength. This is due to the lower crushing strength of those aggregates. The GC20 specimens exhibited lower compressive strength value, which is due to the binder failure and reduction in contact points.

The second hardened property observed in this investigation is split tensile strength, which follows a similar trend of compressive strength. GC specimens exhibited better split tensile strength values than RC specimens. The addition of recycled aggregate in geopolymer concrete significantly reduced the strength values (Peng et al. 2020). At the same time, the reduction in strength values is more than that of RC specimens. This is due to the weak strength of brick aggregate incorporation in geopolymer concrete.

The density of the previous geopolymer concrete ranges from 1418 to 1848. Control specimens are having a density value of 1848 kg/m<sup>3</sup>. The density value of RC is lower than that of the control specimen. Aggregate size has not many effects on the density value of the concrete. The addition of recycled aggregates in the place of natural aggregate significantly reduced the density values due to the adhered mortar present in the recycled aggregates. The incorporation of recycled brick aggregates also reduced the density values; at the same time, aggregate size influences the density values. This is due to the void area reduction in the concrete specimen. From Fig. 6a, compressive strength and density values are linearly related to the slope of 0.0043, and the *R*<sup>2</sup> value is

0.3077. Split tensile strength results follow a similar trend to the compressive strength values. The maximum value of split tensile strength value is observed in the control specimen, and the incorporation of recycled brick aggregates in the place of aggregates reduced the strength properties. The relation between density and compressive strength is shown in Fig. 6a, and the equation formulated for this relationship is Eq. (4)

$$Y = 0.0043x - 1.9527. \quad (4)$$

Figure 6b depicts the split tensile strength results of PGC contain RC and RB. A maximum split tensile strength is observed in GC20 specimens. The addition of RB and RC in geopolymer concrete reduced the split tensile strength properties. The ratio of compressive to split tensile strength value is 8.02% in GC20 specimens, which is 5 to 6% higher than that of conventional concrete (Tangchirapat et al. 2008). GC exhibited denser properties due to the strong interfacial bonding between aggregates and geopolymer binder than that of an ordinary binder. Soluble silicate in geopolymer concrete also enhanced the geopolymer concrete properties (Sarker 2011).

The concrete specimens are tested at the age of 7 days, and the values are plotted in Fig. 6c, and it is evident that the compressive and split tensile strength values are linearly correlated. The relation between them is explained by the linear equation from the plot. And the equation is Eq. (5)

$$Y = 0.6024x - 0.1598. \quad (5)$$

## 7 Durability Results

### 7.1 Total Void Ratio and Water Permeability Coefficient

The void ratio and water permeability of the GC specimens are calculated by using Eq. (2). The void ratio of the

**Table 3** Hardened state test results of geopolymer concrete

Specimen ID	Compressive strength (MPa)			Split tensile strength (MPa)			Split tensile and compression strength ratio 28 days	Density (kg/m <sup>3</sup> )
	7 Days	14 Days	28 Days	7 Days	14 Days	28 Days		
GC6	1.473	3.54	4.49	1.048	1.215	1.321	2.91	1848
GC12	2.04	6.86	7.59	1.332	1.443	1.644	4.62	1830
GC20	5.05	5.09	6.01	1.004	1.2	1.427	3.72	1792
RC6	1.251	2.51	3.95	0.556	0.958	1.014	2.48	1720
RC12	1.987	5.57	6.18	1.221	1.321	1.21	3.70	1735
RC20	3.245	4.25	5.11	0.352	0.725	1.002	3.06	1710
RB6	0.952	2.117	3.21	0.452	0.758	1.001	2.11	1420
RB12	1.125	3.98	5.54	1.12	1.003	1.11	3.33	1450
RB20	1.129	2.99	3.95	0.215	0.558	0.997	2.47	1418

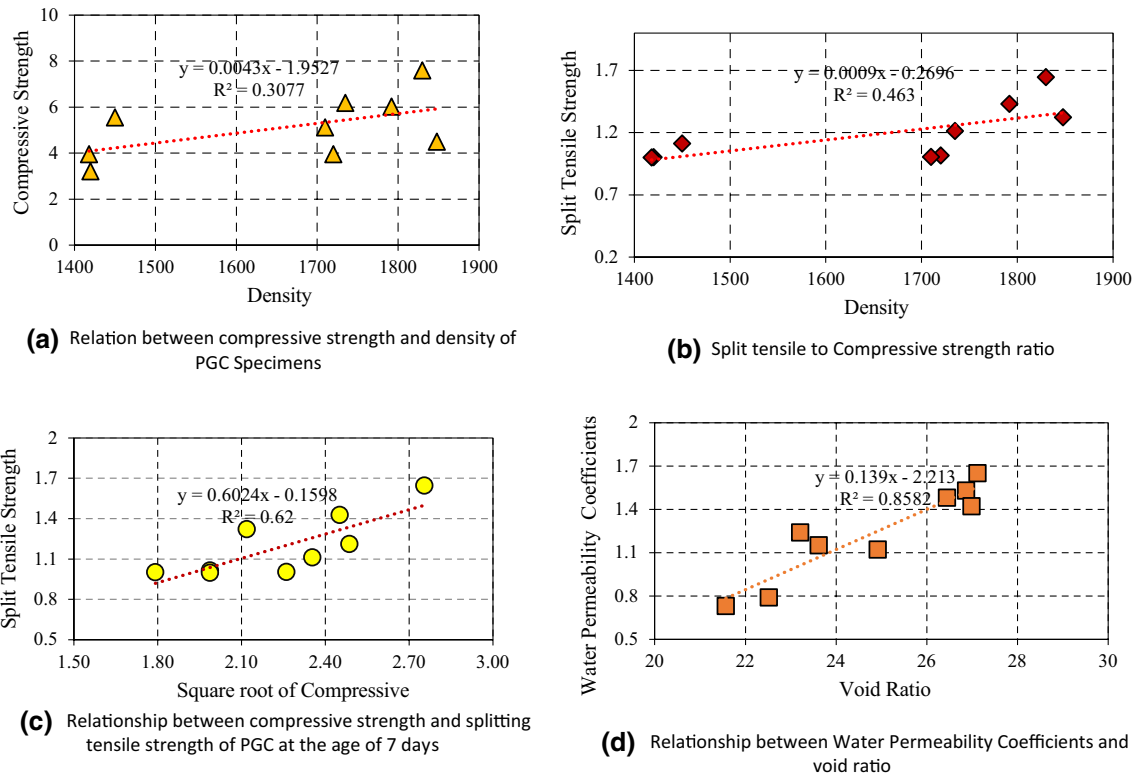


**Fig. 6** **a** Relation between compressive strength and density of PGC specimens. **b** Split tensile-to-compressive strength ratio. **c** Relationship between compressive strength and splitting tensile strength of PGC at the age of 7 days

**d** Relationship between water permeability coefficients and void ratio

GC specimens varied from 23.19% to 28.36%. Void ratios increase with an increase in aggregates size (Tho-in et al. 2012). The relationship between void ratio and permeability coefficient of the specimens (Cetin 2015b) is represented in Fig. 6d. In the case of using RB in PGC, the total void ratios ranged from 21.57 to 27.12.

Water permeability values follow the same trend of the void ratio, which ranges from 0.7 to 1.65. Low permeability values are observed in GC specimens with RC aggregate or RB aggregates. The relation between the void ratio and the permeability values is described by Eq. (6)

$$Y = 0.139x - 2.213. \tag{6}$$

Water absorption results are calculated based on the formula provided in Eq. (3) and listed in Table 4. Figure 7 depicts the results of water absorption values. From the results, it is evident that the incorporation of recycled aggregates boosted the water absorption levels due to the water-absorbing property of recycled aggregates. An increase in aggregate size causes increased water absorption levels due to higher voids present in GC specimens (Celen and Evcin 2020).

Sorptivity results are given in Table 5. Figure 8 illustrates the differences in sorptivity values by using

**Table 4** Water absorption results

Mix ID	Void ratio (%)	Water permeability coefficients (cm/s)	Water absorption
GC6	23.21	1.24	8.24
GC12	24.92	1.12	10.58
GC20	27.12	1.65	11.95
RC6	26.87	1.53	12.12
RC12	26.99	1.42	13.02
RC20	26.45	1.48	14.54
RB6	23.62	1.15	15.2
RB12	21.57	0.73	16.78
RB20	22.52	0.79	17.23

geopolymer concrete recycled aggregate and brick aggregates. Sorptivity value increased in RC and RB specimens due to their water absorption capacity values are high in recycled aggregates compared to normal aggregates (Roslan et al 2021). RCA and RBA aggregate properties specific gravity and density are reduced compared with natural aggregate properties which show voids supplementary in RCA and RBA. Impact value of RCA and RBA are elevated compared with NA, which shows the impact

**Fig. 7** Graphical representation of water absorption

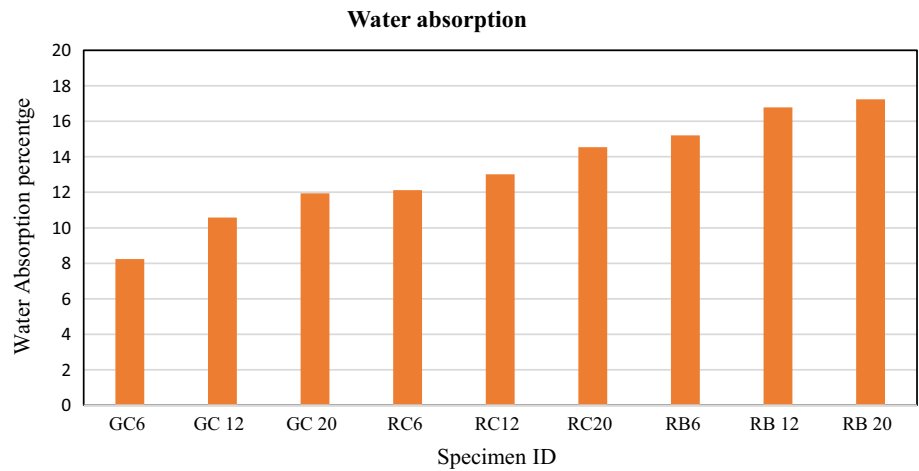


**Table 5** Sorptivity test results

Mix id	30 min	60 min	90 min	120 min
GC6	6.014	6.013	5.174	4.521
GC12	6.16	6.66	5.413	4.67
GC20	6.872	6.873	5.85	4.87
RC6	7.123	7.332	7.554	7.556
RC12	7.032	7.115	7.254	7.361
RC20	7.001	7.325	7.412	7.365
RB6	8.152	8.256	8.736	8.825
RB12	8.223	8.295	8.448	8.225
RB20	8.361	8.378	8.458	8.558

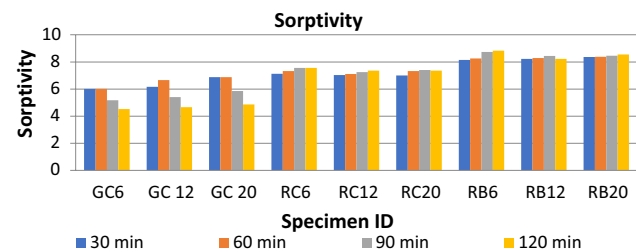


**Fig. 8** Graphical representation of sorptivity test

load-carrying capacity also low for RCA and RBA based on these properties durability of RC and RB decreases compared to GC (Luyt et al 2021).

**Table 6** Test results of beam specimens

Beam	Cracking stage values			Service stage values			Ultimate stage values		
	$P_{cr}$ (kN)	$\Delta_{cr}$	$W_{cr}$	$P_s$ (kN)	$\Delta_s$	$W_s$	$P_u$ (kN)	$\Delta_u$	$W_u$
GC12	43	3.126	0.02	85	5.425	0.16	134	11.325	0.45
RC12	40	2.016	0.02	81	4.156	0.18	103	10.856	0.45
RB12	33	1.535	0.03	65	4.123	0.17	95	9.658	0.37

### 8 Structural Element Fabrication and Testing

At the early stages of loading, there are no cracks visible in the beams. When the load reaches the critical load, the beam gets cracked, further loading increased the cracks, and the crack width also was measured. Typical failure of the beam happens in flexure mode. Deflection occurs at the mid-span of the beam which is considered as a function of load applied toward the beam specimen. The behavior of all the specimens follows the same pattern. The critical load of the beam is notified as  $P_{cr}$ , the deflection of the beam is noted as  $\Delta_{cr}$ , and the crack width at the critical stage of the beam is mentioned as  $W_{cr}$ . Similarly, service stage values and the ultimate stage values are with the subscripts of  $\Delta_s$  and  $\Delta_u$ , respectively.

From Table 6, it is evident that the cracking loads of the beam specimens are reduced by adding RCA and RBA in the place of natural aggregates in geopolymer concrete. The cracking loads vs. deflection patterns are depicted in Fig. 9a, b and c. During the loading of the specimens, all beams follow the same degradation curves. The total deformation of beam specimens and crack width maximum of 10 mm which shows low impact strength value of recycled aggregate, so crack width is high. The cracking load of the beam specimen is noted by measuring the load value at which the first crack formed, and the ultimate load is a load at which the beam failed. Compared with GC beam specimens without recycled



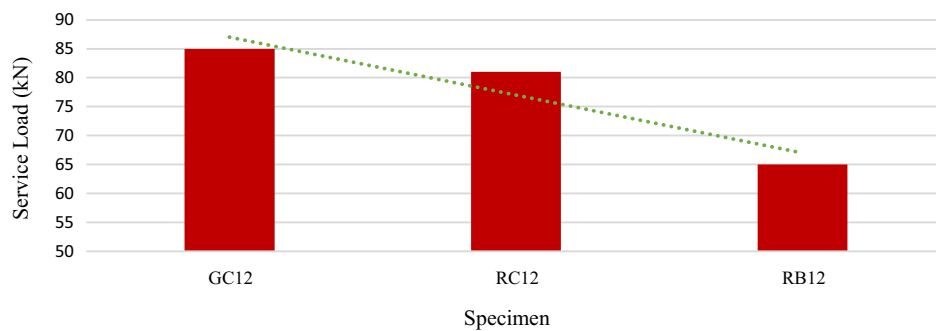
aggregate, GC beam specimens incorporated with recycled aggregate exhibited reduced cracking, highest service, and ultimate load. This is due to the properties of recycled aggregates in beam specimens.

### 9 Evaluation of PGC Beam Specimens using ANSYS

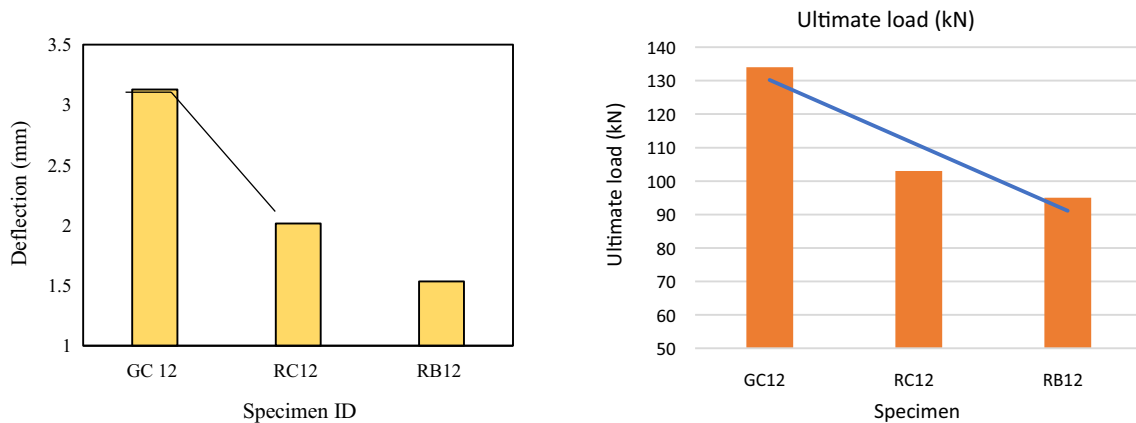
ANSYS is civil engineering software that is used to evaluate the properties of structural elements without performing experimental investigations. The following results are attained from the ANSYS. The results are represented in

Table 7, which provides the ANSYS results of beam specimens, which is close to that of experimental values.

Comparison of charts represented the variation between experimental and analytical results (Kulali 2020). Cracking, service, and ultimate load values are depicted in Fig. 10a, b, and c, which shows the analysis results. Figure 11 shows the deflection of cracking stage, service stage, and ultimate stage beam, which shows deviation within the range of  $-4.09\%$ – $4.56\%$  within the allowable limit of 5%. Figures 12, 13, and 14 show the load of cracking stage, service stage, and ultimate stage beam, which shows  $-3.16\%$ – $1.65\%$  deviation range compared to analysis and experimental results, and it is evident that the variations between the experimental and analytical results are negligible.



(a) Cracking deflection of beam specimens



(b) Cracking deflection of beam specimens

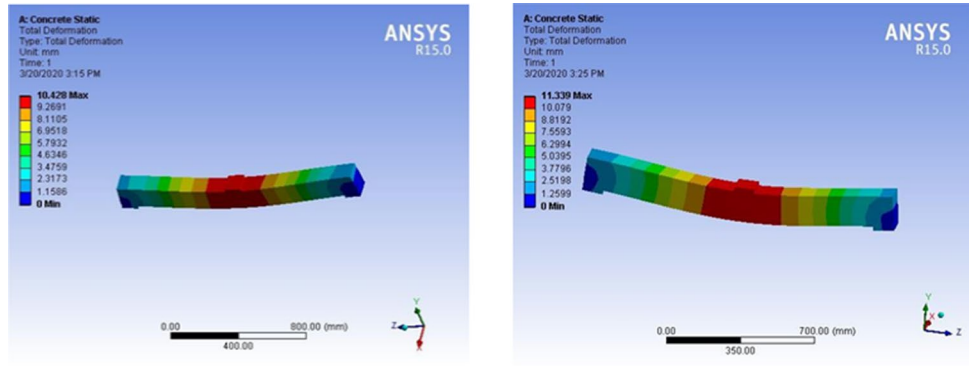
(c) Ultimate Load of beam specimens

Fig. 9 a Cracking deflection of beam specimens. b Cracking deflection of beam specimens. c Ultimate load of beam specimens

Table 7 ANSYS validation of results

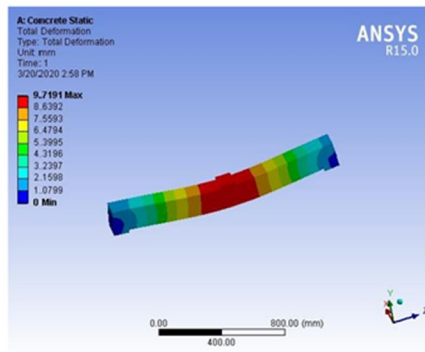
Beam	Cracking stage values			Service stage values			Ultimate stage values		
	$P_{cr}$ (kN)	$\Delta_{cr}$	$W_{cr}$	$P_s$ (kN)	$\Delta_s$	$W_s$	$P_u$ (kN)	$\Delta_u$	$W_u$
GC12	43.02	3.014	0.024	83.6	5.365	0.175	136	11.339	0.45
RC12	40.21	2.007	0.021	80.2	4.326	0.184	105	10.428	0.45
RB12	32.65	1.465	0.037	65.25	4.265	0.169	98	9.658	0.37

Fig. 10 Total deformation



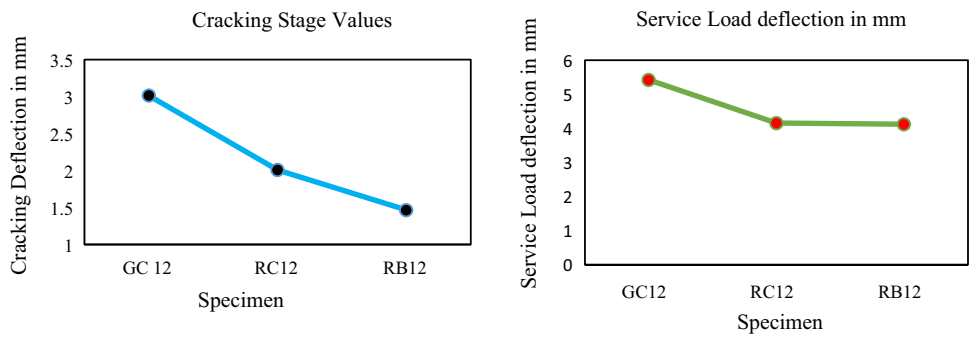
(a) Total Deformation of Beam GC 12

(b) Total Deformation of Beam RC12



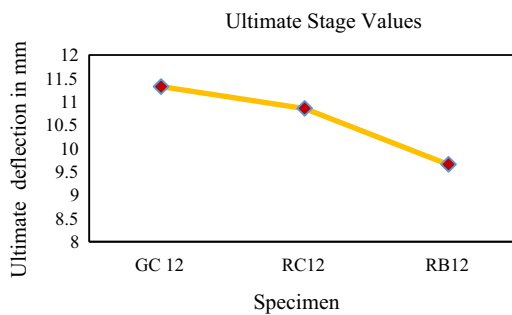
(c) Total Deformation of Beam RB12

Fig. 11 a Cracking stage value. b Service stage values. c Ultimate stage values



(a) Cracking Stage Value

(b) Service Stage Values



(c) Ultimate Stage Values

## 10 Conclusions

The feasibility of using recycled aggregate and recycled brick aggregate in geopolymer concrete has been analyzed, and the following conclusions are drawn:

- The results of these investigations suggested that the incorporation of recycled concrete aggregates and brick aggregates reduced the strength properties; at the same time, the reduction in strength is an acceptable range.
- Alkali activator in geopolymer concrete plays a vital role in the strength properties, and aggregate size plays a significant role in permeability properties.
- The above-mentioned results suggested that the incorporation of recycled concrete aggregates and brick aggregates in geopolymer concrete provides an acceptable range of reduction in the strength properties.
- The compressive strength of GC12, RC12, and RB12 is 7.59, 6.18, and 5.54, respectively. The compressive strength value of RC12 is 19% less than that of GC12 and 27% less than that of RB12.

Comparison of experimental and ANSYS results of Critical Load

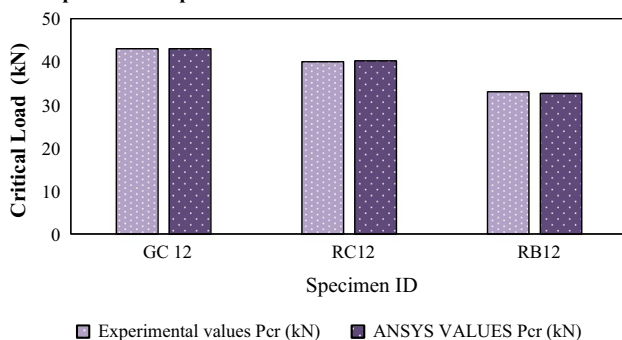


Fig. 12 Comparison of experimental and ANSYS results of critical load

Comparison of experimental and ANSYS results of Service Load

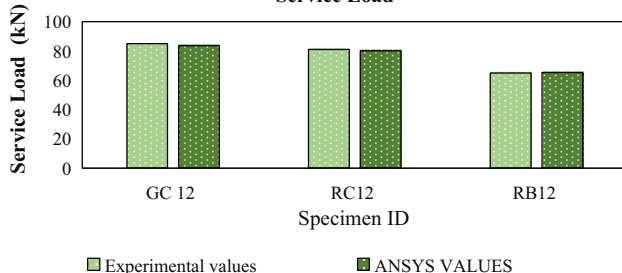


Fig. 13 Comparison of experimental and ANSYS results of service load

Comparison of experimental and ANSYS results of Ultimate Load

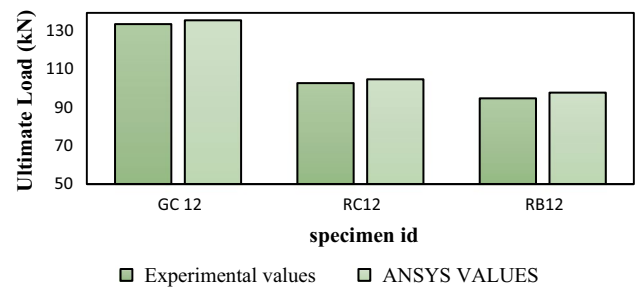


Fig. 14 Comparison of experimental and ANSYS results of ultimate load

- Similarly, the tensile strength of RC12 and RB12 is reduced to 26% and 32% compared to GC12 specimens. The reduction ranges between 12 and 32%, which is an acceptable range of reductions. The ratios of tensile strength to compressive strength ranged from 2.10 to 3.69, which were significantly higher than standard concrete.
- Due to the high void ratio, GC densities were lower between 1418 and 1720 kg/m<sup>3</sup>, which were approximately 23 percent lower than those of conventional geopolymer concrete.
- The void ratio of RC12 and RB12 is 26.99 and 21.57, respectively, which is 8.3% and 13% higher than that of GC12 specimens.
- Geopolymer concrete beam specimens are without using recycled aggregates having higher  $P_{cr}$ ,  $P_s$ , and  $P_u$  than that of PGC with recycled aggregates. The cracking load of the RC12 beam is 6% less than that of the GC12 beam due to the incorporation of recycled concrete aggregate.
- Service loads and ultimate load of RC12 are reduced to 4.9% and 23%, respectively. In RB12 beams, the cracking load is 23% less than that of the GC12 beam. The service and ultimate loads are reduced to 23% and 29%, respectively.
- The observations made in this investigation suggested that the strength properties of structural elements reduced due to the incorporation of recycled concrete and brick aggregate in geopolymer concrete; at the same time, the reduction always lies in acceptable ranges. Validation using ANSYS software is beneficial to understand the behavior of structural elements constructed using geopolymer concrete, and the analytical results are very closer to the experimental values.

## References

- Akbarnezhad A, Nadoushani ZSM (2015) A computational method for selection of optimal concrete recycling strategy. *Mag Concr Res* 67(11):543–558. <https://doi.org/10.1680/mac.14.00211>
- Akbarnezhad A et al (2013) Effects of the parent concrete properties and crushing procedure on the properties of coarse recycled concrete aggregates. *J Mater Civ Eng* 25(12):1795–1802. [https://doi.org/10.1061/\(ASCE\)MT.1943-5533.0000789](https://doi.org/10.1061/(ASCE)MT.1943-5533.0000789)
- Akkurt I, Akyıldırım H (2012) Radiation transmission of concrete including pumice for 662, 1173 and 1332 keV gamma rays. *Nucl Eng Des* 252:163–166. <https://doi.org/10.1016/j.nucengdes.2012.07.008>
- Akkurt I, Basyigit C, Kilincarslan S, Mavi B, Akkurt A (2006) Radiation shielding of concretes containing different aggregates. *Cement Concr Compos* 28(2):153–157. <https://doi.org/10.1016/j.cemconcomp.2005.09.006>
- Akkurt I, Akyıldırım H, Mavi B, Kilincarslan S, Basyigit C (2010) Photon attenuation coefficients of concrete includes barite in different rate. *Ann Nucl Energy* 37(7):910–914. <https://doi.org/10.1016/j.anucene.2010.04.001>
- ASTM C642–13 (2013) Standard Test Method for Density, Absorption, and Voids in Hardened Concrete; ASTM International, 100 Barr Harbor Drive, PO Box C700, West Conshohocken, PA 19428–2959. United States. <http://www.astm.org/cgi-bin/resolver.cgi?C642>
- Babu MA, Babu CR (2017) Mechanical properties of geopolymer pervious concrete. *Int J Civ Eng Technol* 9:2394–2400
- Çelen YY, Evcin A (2020) Synthesis and characterizations of magnetite–borogypsum for radiation shielding. *Emerg Mater Res* 9(3):770–775. <https://doi.org/10.1680/jemmr.20.00098>
- Çelen YY, Evcin A, Akkurt I, Bezir NÇ, Günoğlu K, Kutu N (2019) Evaluation of boron waste and barite against radiation. *Int J Environ Sci Technol* 16(9):5267–5274. <https://doi.org/10.1007/s13762-019-02333-3>
- Cetin M (2013) Landscape engineering, protecting soil, and runoff storm water. Chapter 27, in book: *InTech-open science-open minds*, book: *advances in landscape architecture-environmental sciences*, Eds: Murat Ozyavuz. Online July 1st, 697. <https://www.intechopen.com/books/advances-in-landscape-architecture/landscape-engineering-protecting-soil-and-runoff-storm-water>. <https://doi.org/10.5772/55812>
- Cetin M (2015a) Chapter 55: Using recycling materials for sustainable landscape planning, environment and ecology at the beginning of 21st century, ST. Kliment Ohridski University Press, Sofia, 978–954–07–3999–1, chapter page: 783–788. <https://doi.org/10.13140/RG.2.1.1427.0481>
- Cetin M (2015b) Consideration of permeable pavement in landscape architecture. *J Environ Prot Ecol* 16(1):385–392
- Chindaprasirt P, Chalee W (2014) Effect of sodium hydroxide concentration on chloride penetration and steel corrosion of fly ash-based geopolymer concrete under marine site. *Constr Build Mater* 63:303–310. <https://doi.org/10.1016/j.conbuildmat.2014.04.010>
- Cochran K et al (2007) Estimation of regional building-related C&D debris generation and composition: case study for Florida. *US Waste Manage* 27(7):921–931. <https://doi.org/10.1016/j.wasman.2006.03.023>
- Davidovits J (1991) GEOPOLYMERS inorganic polymeric new materials. *J Therm Anal* 37:1633–1656. <https://doi.org/10.1007/BF01912193>
- Debieb F, Kenai S (2008) The use of coarse and fine crushed bricks as aggregate in concrete. *Constr Build Mater* 22(5):886–93. <https://doi.org/10.1016/j.conbuildmat.2006.12.013>
- Duxson P, Provis JL, Lukey GC, Van Deventer JS (2007) The role of inorganic polymer technology in the development of ‘green concrete.’ *Cem Concr Res* 37(12):1590–1597. <https://doi.org/10.1016/j.cemconres.2007.08.018>
- EN 13755 (2008) Natural stone test methods—Determination of water absorption at atmospheric pressure. <https://doi.org/10.1111/are.13755>
- Etcheberria M, Mari A, Vazquez E (2007) Recycled aggregate concrete as structural material. *Mater Struct* 40(5):529–541
- Ghafoori N, Dutta S (1995) Pavement thickness design for no-fines concrete parking lots. *J Trans Eng* 121(6):476–84. [https://doi.org/10.1061/\(ASCE\)0733-947X\(1995\)121:6\(476\)](https://doi.org/10.1061/(ASCE)0733-947X(1995)121:6(476))
- IS 2386-3 (1963) Indian standard methods of tests for aggregates for concrete, Bureau of Indian Standards, New Delhi, India
- IS 3085 (1965) Methods of test for permeability of cement mortar and concrete (seventh revision). Reaffirmed–Dec 2016
- IS 5816 (1999) Method of test for splitting tensile strength of concrete. Bureau of Indian Standards, New Delhi, India
- IS 516 (1959) Indian standard methods of tests for strength of concrete, Bureau of Indian Standards, New Delhi, India
- Khalaf FM, DeVenny AS (2004) Recycling of demolished masonry rubble as coarse aggregate in concrete: review. *J Mater Civ Eng* 16(4):331–40. [https://doi.org/10.1061/\(ASCE\)08991561\(2004\)16:4\(331\)](https://doi.org/10.1061/(ASCE)08991561(2004)16:4(331))
- Khalaf FM, DeVenny AS (2005) Properties of new and recycled clay brick aggregates for use in concrete. *J Mater Civ Eng* 17(4):456–64. [https://doi.org/10.1061/\(ASCE\)08991561\(2005\)17:4\(456\)](https://doi.org/10.1061/(ASCE)08991561(2005)17:4(456))
- Kilincarslan S, Akkurt I, Basyigit C (2006) The effect of barite rate on some physical and mechanical properties of concrete. *Mater Sci Eng A* 424(1–2):83–86. <https://doi.org/10.1016/j.msea.2006.02.033>
- Kulali F (2020) Simulation studies on the radiological parameters of marble concrete. *Emerg Mater Res* 9(4):1341–1347. <https://doi.org/10.1680/jemmr.20.00307>
- Limbachiya MC, Leelawat T, Dhir RK (2000) Use of recycled concrete aggregate in highstrength concrete. *Mater Struct* 33(11):574–580. <https://doi.org/10.1007/BF02480538>
- Limbachiya M, Meddah MS, Ouchagour Y (2012) Use of recycled concrete aggregate in fly-ash concrete. *Constr Build Mater* 27(1):439–49. <https://doi.org/10.1016/j.conbuildmat.2011.07.023>
- Lotfy A, Al-Fayez M (2015) Performance evaluation of structural concrete using controlled quality coarse and fine recycled concrete aggregate. *Cem Concr Compos* 61:36–43. <https://doi.org/10.1016/j.cemconcomp.2015.02.009>
- Luyt AS, Gasmı SA, Aljindi RM, Ouederni M, Vouyiouka SN, Porfyris AD, Pfaendner R, Papaspyrides CD (2021) Artificial weathering and accelerated heat aging studies on low-density polyethylene (LDPE) produced via autoclave and tubular process technologies. *eXPRESS Polym Lett* 15(2):121–136. <https://doi.org/10.3144/expresspolymlett.2021.12>
- Malayali AB, Chokkalingam RB, Singh MV (2019) Experimental study on the compressive strength and permeable properties of GGBS based geopolymer pervious concrete. *IOP Conf Ser Mater Sci Eng* 561(1):012004. <https://doi.org/10.1088/1757-899X/561/1/012004>
- Malayali AB, Chokkalingam RB, Krishnan TH, Nagaselvam PIOP (2020) Effect of molar content on GGBS based geopolymer pervious concrete. *IOP Conf Ser Mater Sci Eng* 872(1):012146. <https://doi.org/10.1088/1757-899X/872/1/012146>
- Malhotra VM, Mehta PK (2002) High-performance, high-volume fly ash concrete: materials, mixture proportioning, properties, construction practice, and case histories. Canada. <https://www.osti.gov/etdeweb/biblio/20464963>
- Mavi B, Akkurt I (2010) Natural radioactivity and radiation hazards in some building materials used in Isparta. *Turk Radiat Phys Chem*

- 79(9):933–937. <https://doi.org/10.1016/j.radphyschem.2010.03.019>
- McDonald B (1996) RECON waste minimization and environmental program. In: Proceedings of CIB commission meetings and presentations, RMIT, Melbourne, Australia
- Mehta PK (2001) Reducing the environmental impact of concrete. *Concr Int* 23(10):61–66
- Neithalath N, Weiss J, Olek J (2006) Characterizing enhanced porosity concrete using electrical impedance to predict acoustic and hydraulic performance. *Cem Concr Res* 36:2074–85. <https://doi.org/10.1016/j.cemconres.2006.09.001>
- Noushini A, Castel A (2016) The effect of heat-curing on transport properties of lowcalcium fly ash-based geopolymer concrete. *Constr Build Mater* 112:464–477
- Peng K, Qiao H, Chen K (2020) Study on corrosion of reinforcement bars in ceramic recycled gradient concrete. *Emerg Mater Res* 9(1):213–219. <https://doi.org/10.1680/jemmr.19.00073>
- Poon CS, Shui ZH, Lam L (2004) Effect of microstructure of ITZ on compressive strength of concrete prepared with recycled aggregates. *Constr Build Mater* 18(6):461–8
- Roslan N, Rahim SZA, Abdellah AEH, Abdullah MMAB, Błoch K, Pietrusiewicz P, Nabałek M, Szmidla J, Kwiatkowski D, Vasco JOC, Saad MNM, Ghazali MF (2021) Optimisation of shrinkage and strength on thick plate part using recycled LDPE Materials. *Materials* 14:1795
- Sarker PK (2011) Bond strength of reinforcing steel embedded in fly ash-based geopolymer concrete. *Mater Struct* 44(5):1021–1030. <https://doi.org/10.1617/s11527-010-9683-8>
- Schaefer VR, Wang K, Suleiman MT, Kevern J (2006) Mix design development for pervious concrete in cold climates. Technical report. National Concrete Pavement Technology Center, Iowa State Univ, Ames, Iowa. <https://www.perviouspavement.org/downloads/Iowa.pdf>
- Somna K et al (2011) NaOH-activated ground fly ash geopolymer cured at ambient temperature. *Fuel* 90(6):2118–2124. <https://doi.org/10.1016/j.fuel.2011.01.018>
- Tangchirapat W, Buranasing R, Jaturapitakkul C, Chindaprasirt P (2008) Influence of rice husk–bark ash on mechanical properties of concrete containing high amount of recycled aggregates. *Constr Build Mater* 22(8):1812–9. <https://doi.org/10.1016/j.conbuildmat.2007.05.004>
- Tennis P, Leming M, Akers D (2004) Pervious concrete pavements. Skokie, IL: Portland Cement Association. [https://www.researchgate.net/publication/242722509\\_Pervious\\_Concrete\\_Pavements](https://www.researchgate.net/publication/242722509_Pervious_Concrete_Pavements)
- Tho-in T, Sata V, Chindaprasirt P, Jaturapitakkul C (2012) Pervious high-calcium fly ash geopolymer concrete. *Constr Build Mater* 30:366–371. <https://doi.org/10.1016/j.conbuildmat.2011.12.028>
- US Environmental Protection Agency (USEPA) (2009) Estimating 2003 building related construction and demolition materials amounts. EPA530-R-09-002, Washington, DC, USA
- Varol T, Emir T, Akgul M, Ozel HB, Acar HH, Cetin M (2020) Impacts of small-scale mechanized logging equipment on soil compaction in forests. *J Soil Sci Plant Nutr* 20(3):953–963. <https://doi.org/10.1007/s42729-020-00182-5>
- Venkatesan RP, Pazhani KC (2016) Strength and durability properties of geopolymer concrete made with ground granulated blast furnace slag and black rice husk ash. *KSCE J Civ Eng* 20(6):2384–2391. <https://doi.org/10.1007/s12205-015-0564-0>
- Wen SY, Qiao HX, Wang PH, Yang TX, Yang ZQ (2019) Electrochemical characteristic analysis of corrosion of coated steel bars in magnesium oxychloride concrete. *Emerg Mater Res* 8(4):696–703. <https://doi.org/10.1680/jemmr.19.00055>
- Xiao JZ, Li WG, Poon CS (2012) Recent studies on mechanical properties of recycled aggregate concrete in China—a review. *Sci China Technol Sci* 55(6):1463–1480. <https://doi.org/10.1007/s11431-012-4786-9>
- Yang J, Du Q, Bao Y (2011) Concrete with recycled concrete aggregate and crushed clay bricks. *Constr Build Mater* 25(4):1935–45. <https://doi.org/10.1016/j.conbuildmat.2010.11.063>
- Yuan HP et al (2012) A dynamic model for assessing the effects of management strategies on the reduction of construction and demolition waste. *Waste Manage* 32(3):521–531. <https://doi.org/10.1016/j.wasman.2011.11.006>